Theoretical Study of the Primary Processes in the Thermal Decomposition of Hydrazinium Nitroformate

Vitaly G. Kiselev* and Nina P. Gritsan

Institute of Chemical Kinetics and Combustion, Siberian Branch of the Russian Academy of Sciences, 3 Institutskaya Street, 630090 Novosibirsk, Russia, and Novosibirsk State University, 2 Pirogova Street, 630090 Novosibirsk, Russia

Received: July 20, 2009; Revised Manuscript Received: August 27, 2009

The primary reactions of the thermal decomposition of hydrazinium nitroformate (HNF) as well as ammonium nitroformate (ANF) were investigated theoretically using the G3 multilevel procedure. Calculations were performed for the reactions in the gas phase and in the melt using a simplified model of the latter. The influence of the melt on the reaction barriers was taken into account by calculation of the solvation free energies using a PCM model. In contrast with many other energetic salts, the ionic salt structures of the HNF and ANF were found to be minima on the PES. However, the most energetically favorable structures of the HNF and ANF in the gas phase are H-bonded complexes. In the melt, on the contrary, the ionic structure is lowest in free energy because of solvation effects. In both the gas phase and melt, the HNF decomposes preferably to nitroform and hydrazine. This fact agrees well with the experimentally observed absence of HNF among the gas-phase decomposition products. Thermolysis of HNF occurs mainly through the intermediacy of nitroform; computations do not support the suggestion that the aci-nitroform is an important intermediate of HNF thermolysis. The primary dissociation reactions of ANF resemble those of the HNF.

Introduction

Energetic salts containing hydrazinium and ammonium cations (e.g., ammonium perchlorate, ammonium dinitramide) have been widely studied so far.[1−11] An extensive experimental and theoretical study of the energetic salts is directed toward the development of new "green" chlorine-free oxidizers.[12−14] A better understanding of the fundamental nature of these salts would be valuable for finding ways of modifying them and enhancing their properties. Proton transfer and the effect of hydrogen bonding was found to be important in ammonium salts, especially the conversion of ion pairs in the condensed phase to neutral pairs upon sublimation or evaporation (dissociative vaporization).[15−18]

Hydrazinium nitroformate $[C(NO_2)_3]^-[N_2H_5]^+$ (HNF), a salt of nitroform (trinitromethane, **1**) and hydrazine (N_2H_4, **3**), is of significant interest as a component of promising high-performance solid rocket propellants and environmentally "clean" chlorine-free oxidizer. For the first time, the HNF-based propellants were investigated in some detail in the 1960s,[19−25] but the research program was terminated, primarily because of the low stability of this compound and hazardous methods of its synthesis. The interest in HNF was revived in the late 1970s[26−38] when safe synthetic procedures and efficient stabilizers and binders were found.[27,28,32,39,40]

The standard state of HNF is crystalline; its melting point is ∼125 °C.[37,41] In early studies,[24,25] the NO_2 release immediately after melting of the monopropellant HNF was detected using the simple analytical techniques. It was proposed[24] that in the melt, NO_2 radical is the primary product of HNF decomposition, and it reacts with the hydrazine component of HNF according to Scheme 1. Moreover, the C-NO_2 bond rupture was proposed[24] as a primary reaction of the subsequent nitroform thermal decomposition. The HNF decomposition cycle is sustained by newly formed NO_2 molecules.

SCHEME 1

$$(N_2H_5)^+(C(NO_2)_3)^- \longrightarrow (N_2H_5)^+(C(NO_2)_2)^{\bullet -} + \dot{N}O_2$$
$$2\ \dot{N}O_2 + HNF \longrightarrow N_2O + NH_4NO_3 + CH(NO_2)_3$$

SCHEME 2

$$3\ HNF_{(sol.)} \longrightarrow 2\ NH_4C(NO_2)_3 + 2\ H_2O + N_2 + 2\ N_2O + [CH_3NO_2]$$

SCHEME 3

$$HNF \longrightarrow \underset{\mathbf{1}}{(CH(NO_2)_3)_{gas}} + \underset{\mathbf{3}}{(N_2H_4)_{gas}}$$

Later,[26] Koroban et al. investigated thermolysis of polycrystalline HNF at 70−100 °C. Ammonium nitroformate (ANF), N_2, N_2O, and H_2O were detected as the primary decomposition products. The C-NO_2 bond cleavage was also suggested as a primary reaction. The effective activation energy of the initial stage of decomposition process was found to be 43 kcal/mol. On the basis of the chromatographic product analysis, the following scheme of the solid-state thermolysis was proposed (Scheme 2).[26] The term in square brackets corresponds to the stoichiometry of the proposed residue.

Note that the strong dependence of the HNF decomposition rate on the vessel innage (m/V) has been observed.[26] This fact was proposed to be the evidence of the dissociative vaporization of HNF (Scheme 3).[42]

Williams and Brill[30,31] have studied the thermal decomposition of the HNF in the temperature range 25−400 °C by means of T-jump/FTIR technique. At temperatures below the melting point (125 °C), only very slow decomposition was observed. According to the IR spectroscopy, the only detectable solid product was NH_4NO_3. No evidence of ANF intermediacy in the thermolysis of polycrystalline samples was found. This fact contradicts Koroban's results.[26] In the temperature range

* To whom correspondence should be addressed. Tel: 7 (383) 333 3053. Fax: 7 (383) 330 7350. E-mail: vitaly.kiselev@kinetics.nsc.ru.

10.1021/jp906853e CCC: $40.75
Published on Web 09/17/2009

SCHEME 4

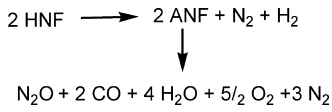

SCHEME 5

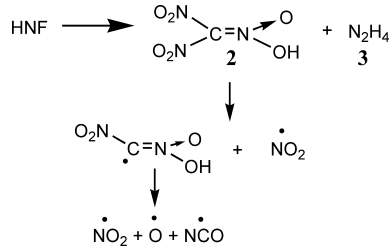

SCHEME 6

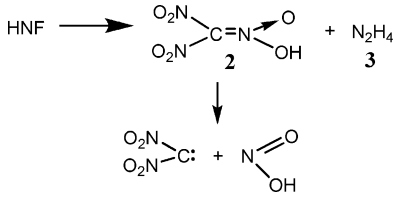

125−260 °C, **1**, **3**, N_2O, H_2O, CO, and ANF aerosol were detected in the gas phase; no traces of HNF, gas, or aerosol, were found. The following idealized reaction pathway (although a bit speculative because N_2 and H_2 are IR-inactive) for decomposition in the melt has been proposed (Scheme 4). The formation of **1** and **3** was attributed to the dissociative vaporization of HNF (Scheme 3).[26] In contrast with the previous results,[24,25] NO_2 formation had not been detected.

At temperatures above 260 °C, the rates of gasification and heating accelerated so rapidly that deflagration took place.[30,31] The formation of CO_2 was observed for the first time, and its amount increased with the growth of temperature, whereas ANF, N_2O, and CO were not detected at temperatures above 350 °C.

Sinditskii et al.[43,44] performed a thermocouple study of HNF combustion. According to the measured temperature profiles, two distinguishable zones exist in the HNF flame. On the basis of the pressure dependence of the burning surface temperature, the enthalpy of HNF vaporization was found to be 36.3 kcal/mol. In contrast with the previous assumptions,[24,30,31] the authors proposed that the primary reaction of HNF decomposition in the melt is the formation of aci-form **2**, followed by the C-NO_2 bond scission (Scheme 5). In the meantime, the main gas-phase products of HNF dissociative vaporization were proposed to be **1** and **3** (Scheme 3).[30,31,44]

Louwers et al.[37,45] have studied the combustion of HNF in "hot-cell" and "hot-plate" experiments in the temperature range 130−300 °C using the UV-absorption spectroscopy. HONO and NO_2 were the main detectable products; some HNF (vaporized or aerosol) was detected as well. In accordance with Sinditskii's assumption,[43,44] the authors proposed the aci-form **2** to be the primary intermediate of the HNF decomposition. However, dinitrocarbene and nitrous acid were suggested to be the main products of the aci-form **2** decomposition (Scheme 6). The decay of the dinitrocarbene was proposed to lead primarily to NO_2 and CO_2 species.[37,45]

Because the primary products have not been detected, the proposed mechanisms are to some extent speculative. Moreover, a number of different pathways and key intermediates of the HNF thermal decomposition have been suggested, but they were not sufficiently supported and substantiated. Furthermore, the existing experimental data on the decomposition pathways of **1** and **2** are also scarce. The only paper devoted to the thermolysis of **1** has been published, and the decay of **1** was exclusively attributed to the C-NO_2 bond cleavage.[46] The gas-phase activation energy was estimated to be 42.4 kcal/mol, although the significant contribution of the surface reactions was pointed out. Thermolysis of aci-form **2** has never been studied; nevertheless, two different decomposition reactions have been proposed for **2** (Schemes 5 and 6).[37,43,44]

The thermodynamic characteristics of the HNF and intermediates of its thermal decomposition as well as the rate constants of elementary reactions are crucial for modeling the complex combustion process. The different reactions in the proposed HNF combustion mechanisms[26,42,44,45] have been treated mainly qualitatively, based on the chemical intuition, by analogy to similar reactions and empirical correlations. The quantum chemical calculations are the most appropriate alternative for obtaining the thermodynamic and kinetic properties of HNF decomposition reactions.

Some energetic N,O-containing ionic salts, for instance, ammonium dinitramide (ADN) and ammonium nitrite, have been intensively studied theoretically.[47−49] Proton transfer processes in ammonium and hydroxylammonium nitrates[50,51] in the nitric acid/ammonia system[15,16] and in complexes of hydrogen halides with NH_3 and various amines[17,18] were studied using theoretical methods as well. However, to the best of our knowledge, properties of the HNF and mechanism of its thermolysis have never been studied theoretically at a high level of theory. Only some estimations using semiempirical methods have been made.[37]

The main goal of our article is to give insight into the primary processes of the HNF decomposition in the gas phase and in the melt. Because ANF is a proposed intermediate of HNF thermal decomposition,[26,30,31] the primary processes of its thermolysis were also considered. The structure and thermodynamic properties of HNF and ANF in both the gas phase and melt have been investigated at different levels of theory (up to G3 level). The intermediates of the primary decomposition reactions of HNF have been identified, and the selected decomposition reactions of nitroform **1** and its aci-form **2** were also investigated.

Computational Details

The geometries of the ionic and acid−base HNF structures were optimized at the B3LYP and MP2 levels of theory with the basis sets of different size. The 6-311G(d,p), 6-311++G(2df,p), and 6-311++G(3df,2p) basis sets were used for the B3LYP calculations, and the 6-31G(d) and 6-311++G(d,p) basis sets were employed for the MP2 computations. All equilibrium and transition-state structures were ascertained to be the minima or saddle points, accordingly, on the potential energy surfaces. The intrinsic reaction coordinate (IRC) procedure[52] was employed to make certain that the localized transition states connected the desired reagents and products. The corresponding thermal corrections were included to obtain the enthalpy and Gibbs free energy values at the desirable temperature. Apart from that, the thermodynamic properties of HNF and ANF in the form of ionic salts and acid−base pairs were refined using multilevel technique. Among numerous very accurate multilevel procedures, we chose the G3 method[53] because we had previously demonstrated a good performance of this technique for thermochemical and kinetic calculations of N,O-containing compounds.[54,55]

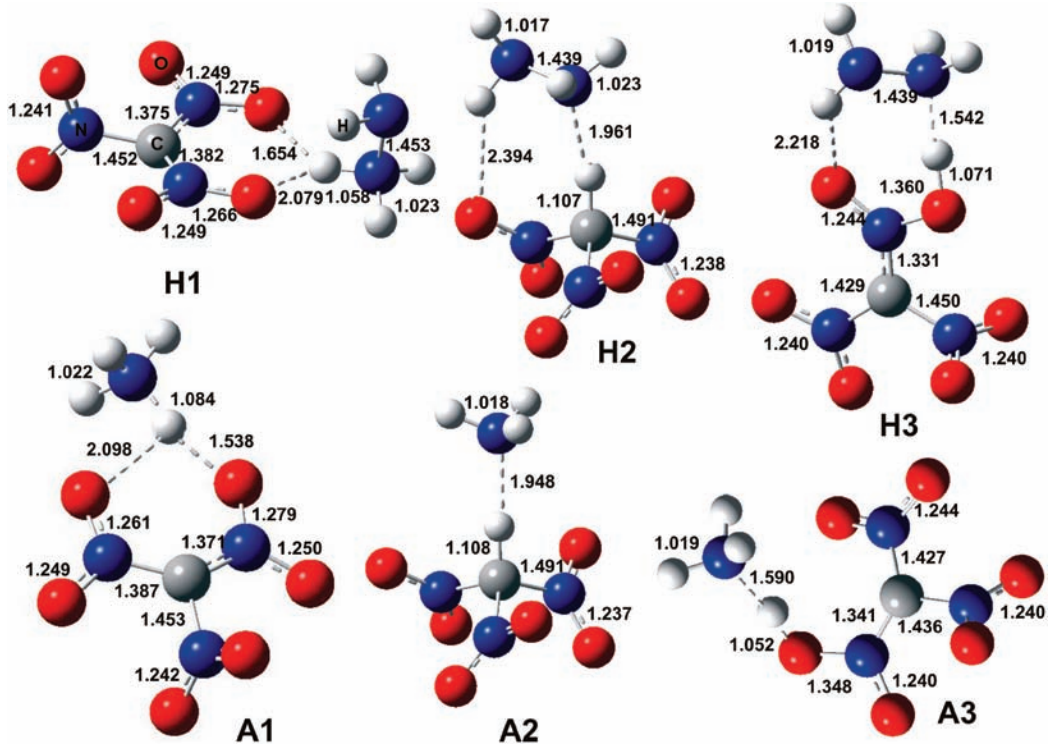

Figure 1. Bond lengths (in angstroms) in different forms (ionic salts and acid−base pairs) of HNF and ANF optimized at the MP2(full)/6-31G(d) level of theory.

The influence of melt on the reaction free energies and free energies of activation was taken into account by calculation of solvation free energies using the PCM model[56,57] at the B3LYP/6-311G(d,p) level of theory.[58,59] Typical polar solvent, acetonitrile, was chosen for our simple model calculations. We hypothesize that this polar solvent can reproduce the solvation of the HNF and ANF salts by the melt fairly well. It is noteworthy that acetonitrile is fully parametrized for the application in the calculations using the PCM model.[56,57] All quantum chemical computations were performed using the Gaussian 03 suite of programs.[60]

The gas-phase enthalpies of formation (at $p = 1$ atm and $T = 298$ K, $\Delta_f H^0_{gas}$) were obtained using the atomization energy approach: the calculated atomization energies at 298 K were subtracted from the well-known enthalpies of formation of the isolated atoms. For any molecule, M, the enthalpy of formation was calculated as follows[61]

$$\Delta_f H^0_{gas}(\mathrm{M}) = E_{el}(\mathrm{M}) + \mathrm{ZPVE}(\mathrm{M}) + [H_{298}(\mathrm{M}) - H_0(\mathrm{M})] - \sum_i^{atoms} \{E_{el}(X_i) + [H_{298}(X_i) - H_0(X_i)]\} + \sum_i^{atoms} \Delta_f H^0_{gas}(X_i)$$

where $E_{el}(\mathrm{M})$ is the electronic energy of the molecule calculated at the chosen level of theory, $E_{el}(X_i)$ is the electronic energy of the atom X_i calculated using the same technique, ZPVE is the energy of molecule's zero-point vibrations, and $[H_{298}(\mathrm{M}) - H_0(\mathrm{M})]$ is a thermal correction to the enthalpy obtained by means of simple Gibbs' statistical mechanics. The NIST-JANNAF tables[62,63] were used as a source of the atomic enthalpies $\Delta_f H^0_{gas}(X_i)$.

Results and Discussion

1. Formation Enthalpies of the Hydrazinium Nitroformate and Ammonium Nitroformate in the Form of Ionic Salts and Acid−Base Pairs and Their Mutual Interconversion. As mentioned in the Introduction, the formation of nitroform (**1**) and hydrazine (**3**) in the gas phase upon thermolysis of HNF was usually attributed to the dissociative vaporization of HNF.[26,30,31,40,42] This means that the ionic structure, $[C(NO_2)_3]^-[N_2H_5]^+$, was hypothesized not to exist in the gas phase. Note that the previous theoretical studies on the ADN[47] and HNO_3-NH_3[15] systems demonstrated that only hydrogen-bonded acid−base complexes could be localized on the potential energy surfaces of these systems.

In contrast with the above-mentioned assumption, we have been able to optimize the ionic structures of HNF and ANF, $[C(NO_2)_3]^-[N_2H_5]^+$ (**H1**) and $[C(NO_2)_3]^-[NH_4]^+$ (**A1**), at the HF, MP2, and B3LYP levels of theory. Figure 1 demonstrates the gas-phase structures of **H1** and **A1** optimized at the MP2(full)/6-31G(d) level of theory (in the framework of the G3 procedure). According to the crystallographic data,[23] there are two types of $C(NO_2)_3^-$ anions and $N_2H_5^+$ cations in the asymmetrical unit of HNF crystal. The calculated bond lengths, bond angles, and dihedral angles in the cation and anion of the ionic structure **H1** (Figure 1) coincide fairly well (within ~0.02 Å, ~2°, and ~5°, respectively) with the data for the second type of anions and cations in the crystallographic unit.[23]

In addition, we optimized for HNF two hydrogen-bonded acid−base structures **H2** and **H3** (Figure 1). The former is the H-bonded complex of nitroform **1** and hydrazine ($CH(NO_2)_3\cdots N_2H_4$) and the latter is the H-bonded complex of aci-nitroform **2** and hydrazine ($C(NO_2)_2NOOH\cdots N_2H_4$). Similar hydrogen-bonded acid−base complexes were optimized for the ANF (Figure 1, **A2** and **A3**). An extensive search showed that **H1**

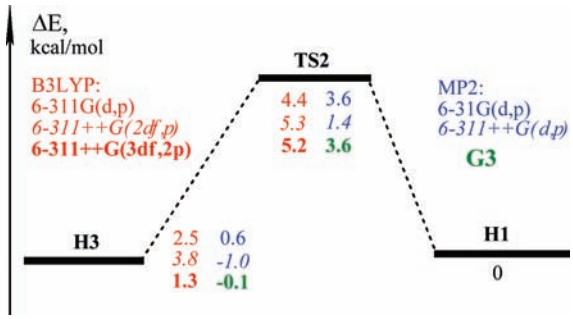

Figure 2. Gas-phase relative electronic energies (ΔE) of the ionic structure of HNF (**H1**), acid−base complex **H3**, and transition state of the proton transfer reaction (**TS2**).

and **A1** are the only ionic structures on the corresponding PES; all attempts to find other ionic structures failed.

To exclude the possibility that the localization of the gas-phase ionic structure **H1** is just an artifact of geometry optimization at a relatively low MP2/6-31G(d) level of theory, we optimized geometries of **H1** and **H3** as well as a transition state for their interconversion using the B3LYP and MP2 methods with different basis sets of increasing size (Figure 2). The results demonstrate that the structures **H1** and **H3** are predicted to be two distinct minima on the PES of HNF at all levels of theory employed, although their energies are close to each other, and the barrier of the proton transfer reaction is quite low. The B3LYP method predicts that the ionic structure is even lower in energy than the acid−base structure **H3**, although the MP2 method with a large basis set predicts that **H3**, on the contrary, is slightly more stable than **H1**. The barrier of the proton transfer reaction predicted by the B3LYP method is a bit higher than that obtained by the MP2 technique. The energy values were refined afterward using the G3 procedure, and the energy levels of **H1** and **H3** were predicted to be almost degenerate.

The calculated and experimental gas-phase formation enthalpies ($\Delta_f H^0_{gas}$) of HNF and ANF in the ionic and acid−base forms and intermediates of their decomposition (**1**−**4**) are presented in Table 1. For the demonstration of reliability of the method employed, this table contains the calculated $\Delta_f H^0_{gas}$ values of nitroalkanes with the well-known experimental enthalpies of formation (**5** and **6**). Note that the accuracy of the experimental formation enthalpies of different nitroalkanes was discussed in detail in ref 54. Only the G3 procedure demonstrated good performance for the calculation of the formation enthalpy of nitromethanes.[54]

Table 1 demonstrates that the calculated $\Delta_f H^0_{gas}$ value agrees well (within 1 kcal/mol) with the experiment for ammonia (**4**). In the case of hydrazine (**3**), the discrepancy between calculated and experimental $\Delta_f H^0_{gas}$ is noticeable (~2 kcal/mol), but the only available experimental value was measured in the fifties.[63] Note that a more reliable value $\Delta_f H^0_{gas} = 23.1$ kcal/mol has recently been calculated for hydrazine at a very high CCSD(T)/CBS level of theory.[68] Nevertheless, the predicted values of $\Delta_f H^0_{gas}$ are in reasonable agreement with experiment for compounds **1** and **4**−**6**. Therefore, one can assume that the G3 method suits reasonably for the present study.

Table 1 also displays the relative gas-phase Gibbs free energies of the ionic and acid−base forms of HNF and ANF. It is seen from Table 1 that in the gas phase, the **H2**, being the H-bonded complex of **1** and **3**, is the most stable structure. **H3**, the H-bonded complex of **2** and **3**, is also slightly more favorable than **H1**.

TABLE 1: Calculated and Experimental Gas-Phase Formation Enthalpies at 298 K ($\Delta_f H^0_{gas}$), the Relative Gas-Phase Gibbs Free Energies at 298 K ($\Delta(\Delta G^0_{gas})$) for the Isomers H1−H3 and A1−A3 Calculated at the G3 Level, and the Free Energies of Solvation (ΔG^0_{solv}) Calculated Using the PCM Model at the B3LYP Level[a,b]

molecule	$\Delta_f H^0_{gas}$	$\Delta_f H^0_{gas}$ (exptl)[c]	$\Delta(\Delta G^0_{gas})$	ΔG^0_{solv}
H1	28.9		0.0	−12.5
H2	16.6		−13.3	3.1
H3	27.5		−1.5	−3.0
A1	−1.6		0.0	−14.6
A2	−17.5		−17.1	3.8
A3	−3.2		−1.5	−3.2
$CH(NO_2)_3$ **1**	1.3	-0.2 ± 0.5[64]		
$C(NO_2)_2NOOH$ **2**	16.4			
N_2H_4 **3**	24.9	22.8[62,63]		
NH_3 **4**	−10.2	−11.0[62,63]		
CH_3NO_2 **5**	−17.5	−17.8[65,66]		
$C(NO_2)_4$ **6**	19.6	19.7 ± 0.5[67]		

[a] **H1** and **A1** ionic forms were chosen as reference compounds for the calculation of the relative thermodynamic properties. [b] All values are in kilocalories per mole. [c] See also a discussion on the most trustworthy experimental $\Delta_f H^0_{gas}$(exptl) values of **1**, **5**, and **6** in ref 54.

It is natural that a single ion pair in the gas phase is significantly less favorable thermodynamically than the H-bonded complex of neutral species **H2**. Likewise, it might be expected that in the condensed phase the ionic salt is more preferable. The previous studies on the ADN and ammonium nitrate systems have shown that even the dimerization of considered species led to proton transfer and made ionic pair thermodynamically more favorable.[48,49]

In the present study, we estimated the stabilization of the **H1** form by calculation of the free energy of solvation in the model solvent using the PCM approach. However, even this simple model correctly predicted the stabilization of the **H1** ionic pair. Figure 3 shows the stationary points on the Gibbs free energy surface (FES) of HNF in the melt. Solvation profoundly stabilizes the highly polar structure **H1**, and it becomes the preferable species among the HNF forms **H1**−**H3**. The free energy of **H1** is 2.4 kcal/mol lower than that of H-bonded complex **H2**. **H3** has noticeably higher free energy than **H1** ($\Delta(\Delta G^0_{melt}) = 8.0$ kcal/mol). The dissociation of **H3** to the neutral species **2** and **3** is a highly endothermic process in the melt ($\Delta(\Delta G^0_{melt}) = 13.2$ kcal/mol). In contrast with the **H1** → **H3** transformation, the free energy of activation for the **H1** → **H2** conversion is lower (8.6 kcal/mol). The products of **H2** decomposition, **1** and **3**, are substantially more stable (by 13.3 kcal/mol) than their counterparts **2** and **3**. The free energy of the whole process (**H1** → **1** + **3**) is predicted to be −0.1 kcal/mol. Therefore, HNF molecule in the melt is prone to fast decomposition to **1** and **3** through the intermediacy of the H-bonded complex **H2**.

The FES of ANF resembles that of the HNF counterpart (Figure S1 in the Supporting Information). In the melt, the salt **A1** is the most stable species, and the H-bonded complex **A3** is much higher in free energy than **A1**. Similar to the HNF case, decomposition of **A1** into **1** and **4** remains more preferable than the dissociation to **2** and **4**. The free energy of the whole process (**A1** → **1** + **4**) equals −0.4 kcal/mol.

Therefore, it is seen that the molten HNF is liable to fast decomposition to **1** and **3** species. This fact agrees well with the absence of HNF among the gas-phase decomposition products, whereas **1** and **3** were detected instead.[30,31,44,45]

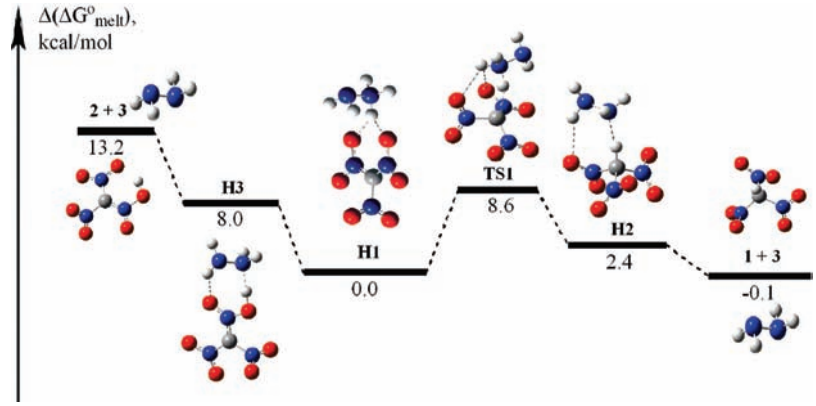

Figure 3. Relative Gibbs free energies ($\Delta(\Delta G^0_{melt})$) of the stationary points on the PES of HNF in the melt. All values are in kilocalories per mole.

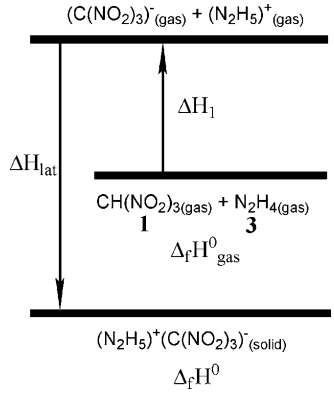

Figure 4. Born−Haber cycle for the estimation of the formation enthalpy of crystalline HNF.

Moreover, experimental data on the sublimation of HNF support this conclusion as well. As mentioned above, the standard state of HNF is the crystal one with $\Delta_f H^0 = -18.4 \pm 0.3$ kcal/mol.[69] The temperature dependence of the HNF vapor has been measured at the temperature range 34.4−67.7 °C[37] and approximated by the Clausius−Clapeyron equation

$$\ln P = -\frac{\beta}{RT} + C \qquad (1)$$

The value of β was found to be 23.2 kcal/mol. If HNF exists in the gas phase mainly in the **H1** form, then β should be equal to the sublimation enthalpy ($\Delta_f H_{subl}$). If HNF undergoes decomposition to two species (**1** and **3**), then β is equal to $\Delta_f H_{subl}$/2. In the first assumption, the gas-phase formation enthalpy of **H1** could be estimated to be 4.8 kcal/mol, which is much smaller than the calculated value 28.9 kcal/mol (Table 1). Using the second assumption, the sum of the gas-phase formation enthalpies of **1** and **3** could be estimated to be 28 kcal/mol. This value agrees well with our calculations (26.2 kcal/mol).

Note that Sinditskii et al.[44] estimated in a similar manner the enthalpy of vaporization of HNF ($\Delta H_{vap} = 36.7$ kcal/mol). Authors analyzed the pressure dependence of the burning surface temperature using eq 1. It was proposed that β is equal to $\Delta H_{vap}/2$.

We also estimated $\Delta_f H^0$ of HNF by means of the Born−Haber thermodynamic cycle (Figure 4). This procedure has been successfully applied for formation enthalpy and stability estimations of a series of energetic ionic salts and liquids.[70]

The most reliable theoretical values of the gas-phase formation enthalpies of **1** and **3** were taken from the literature ($\Delta_f H_{gas}{}^0 = 1.3$ kcal/mol obtained at the G3 level for **1**[54] and 23.1 kcal/mol calculated at the CCSD(T)/CBS level for **3**[68]). The proton transfer enthalpy $\Delta H_1 = 106.8$ kcal/mol was calculated at the G3 level of theory. The lattice enthalpy was estimated using the correlation formula proposed by Jenkins et al.[71,72]

$$\Delta H_{Lat} = 2I(^{\alpha}/_{\sqrt[3]{V}} + \beta) + 2RT \qquad (2)$$

where I is the ionic strength (1.0 in the case of HNF and ANF), V is the molecular volume of the lattice, which is equal to the sum of the cation ($N_2H_5^+$) and anion ($C(NO_2)_3^-$) volumes calculated at the B3LYP level, and α and β are empirical parameters. Using the values $\alpha = 28.0$ (kcal nm)/mol and $\beta = 12.4$ kcal/mol initially derived by Jenkins,[72] we obtained the lattice enthalpy $\Delta H_{lat} = 125.7$ kcal/mol. The corresponding standard state formation enthalpy of HNF was estimated to be $\Delta_f H^0 = 5.5$ kcal/mol in harsh disagreement with the experimental value (−18.4 ± 0.3 kcal/mol).[69]

However, Dixon et al. have recently pointed out[73] an insufficient performance of empirical lattice energy estimations[71,72] for certain classes of compounds. The authors[73] proposed another parametrization ($\alpha = 19.9$ (kcal nm)/mol and $\beta = 37.6$ kcal/mol) particularly for salts containing ammonium, alkylammonium, and hydrazinium cations. In addition, an empirical correction formula was proposed to account for the differences between predicted and experimental total volumes due to flat shapes of the ions.[73] The lattice enthalpy of HNF calculated using these improved parameters is equal to 150.8 kcal/mol, and the estimated formation enthalpy is $\Delta_f H^0 = -19.6$ kcal/mol in perfect agreement with experiment ($\Delta_f H^0 = -18.4 \pm 0.3$ kcal/mol).[69] Nevertheless, it should be noted that such correlation formulas must be handled with care. The authors[73] estimated error bars of their correlation to be 6 to 7 kcal/mol. In the case of ANF, the formation enthalpy $\Delta_f H^0 = -53.9$ kcal/mol estimated in analogous way is a bit further from the only experimental value available $\Delta_f H^0 = -47.3 \pm 0.2$ kcal/mol.[74] However, an agreement between experimental and estimated values is indeed reasonable.

Apart from the Born−Haber cycle consideration, we calculated the enthalpy of proton loss for **1** and the proton affinity of **3** (i.e., $\Delta_r H^0$ for the gas-phase protonation reaction). The value $\Delta_r H^0 = 207.1$ kcal/mol obtained for the proton affinity of **3** agrees well with the value $\Delta_r H^0 = 206.1$ kcal/mol computed earlier at the CCSD(T)/CBS level of theory.[68] The enthalpy of deprotonation of **1** was found to be $\Delta_r H^0 = 313.9$ kcal/mol. Note that the value $\Delta_r H^0 = 303.3$ kcal/mol predicted at the

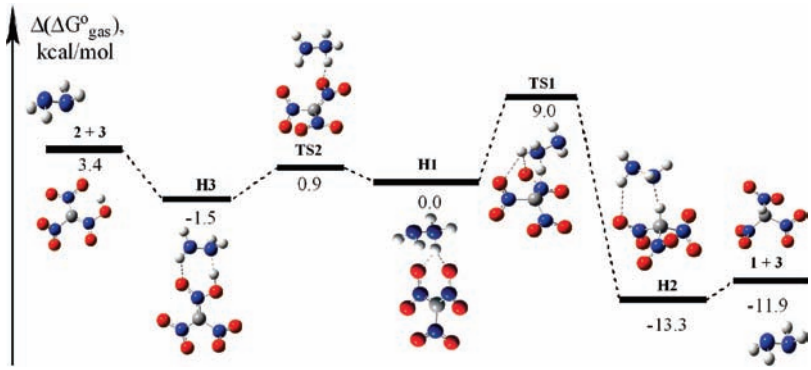

Figure 5. Relative Gibbs free energies in the gas phase at 298 K ($\Delta(\Delta G^0_{gas})$) of the stationary points on the PES for the transformation of HNF. All values are in kilocalories per mole.

B3LYP/6-311+G(d,p) level has been reported.[75] As a good performance of G3 and related procedures for gas-phase acidity calculations have been demonstrated for several compounds with well-established experimental data,[76,77] our value seems to be more robust.

We also considered the possible reactions of HNF decomposition in the gas phase. The stationary points on the gas-phase Gibbs FES of HNF are shown in Figure 5. Similar to the case of melt, the dissociation of the ionic form **H1** to the neutral species **1** and **3** is a two-step process that proceeds through the formation of the H-bonded complex **H2**. The free energy of the whole process is equal to −11.9 kcal/mol.

Figures 2 and 5 also demonstrate that the barrier height for **H1** → **H3** transformation is very low ($\Delta E^{\ddagger} = 3.6$ kcal/mol, $\Delta G^{\ddagger}_{gas} = 0.9$ kcal/mol at the G3 level of theory). Therefore, in the gas phase, **H1** and **H3** are in equilibrium. Because the gas-phase free energies of stationary points were calculated in the harmonic approximation, taking into account anharmonicity effects may lead to the disappearance of low (<1 kcal/mol) activation barriers.

Although the H-bonded complex **H2** is much lower in free energy than **H1** and **H3**, the barrier for the **H1** → **H2** transformation is noticeable (9.0 kcal/mol). However, the free energy of the nitroform **1** and hydrazine **3** is much lower than that of the aci-form **2** and hydrazine **3** (Figure 5). Therefore, the HNF molecule being evaporated may exist in the gas phase, although it is prone to fast decomposition to **1** and **3** through the intermediacy of the H-bonded complex **H2**. Therefore, one may conclude that the main decomposition processes are the same in both the melt and gas phases: the formation of **1** and **3** through the H-bonded complex **H2** is a thermodynamically more favorable process than the formation of **2** and **3** through **H3**.

Figure 1 demonstrates that the structures of the **A1**−**A3** forms of ANF resemble those of HNF (**H1**−**H3**). The results of our calculations for the stationary points on the FES for the transformations of ANF isomers in the gas phase are presented in the Supporting Information (Figure S2). Analogous to the HNF case, a distinctive minimum corresponding to the **A1** ionic structure exists on the PES. The H-bonded complex **A2** was found to be lower in energy than the salt **A1** ($\Delta(\Delta G^0_{gas}) = -17.1$ kcal/mol). Similar to the case of HNF, the dissociation of **A1** to the neutral species **1** and **4** is a two-step process that proceeds through the formation of the H-bonded complex **A2** (Figure S1 in the Supporting Information). The free energy of the whole process is equal to −15.1 kcal/mol.

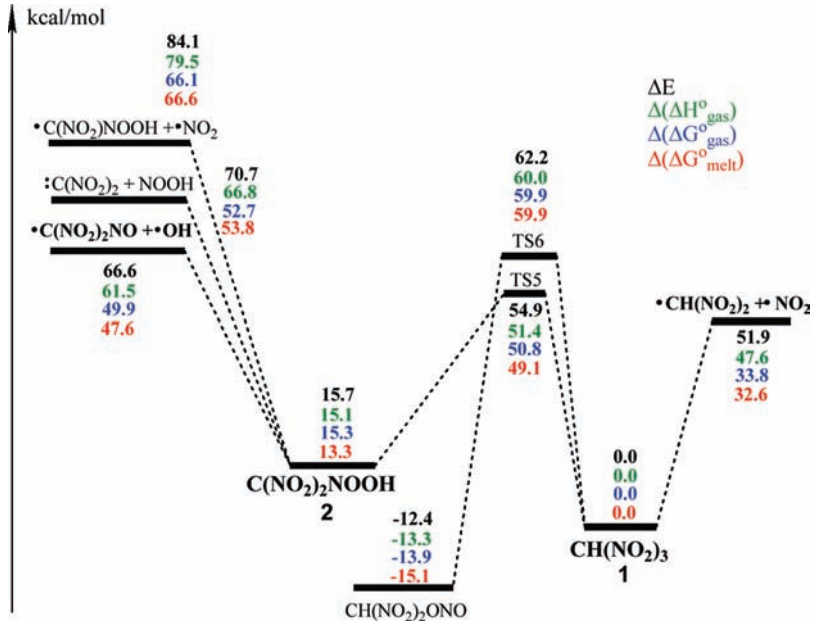

Figure 6. Relative electronic energies (ΔE), enthalpies ($\Delta(\Delta H^0_{gas})$), and Gibbs free energies at 298 K in the gas phase ($\Delta(\Delta G^0_{gas})$) and the melt ($\Delta(\Delta G^0_{melt})$) for the stationary points on the PES of **1** and **2**. All values are in kilocalories per mole.

2. Primary Reactions of the Thermal Decomposition of 1 and 2. Sinditskii et al.[44] and Lowers et al.[37,45] suggested **2** to be the key intermediate of the HNF decomposition in the melt (Schemes 5 and 6). However, our calculations predict that the formation of **1** is even more preferable in the melt than in the gas phase. At the same time, the intermediacy of **2** might be important if its decomposition is significantly faster than that of **1**. Therefore, we studied the primary processes of **1** and **2** thermal decomposition in the melt and in the gas phase.

Figure 6 represents the relative thermodynamic potentials of the stationary points on the PES for the thermal decomposition of **1** and **2**. It is seen that in the gas phase, C−NO_2 bond cleavage dominates for **1**, whereas the N−OH bond scission is the most preferable decomposition reaction of **2**. The NOOH and NO_2 elimination reactions previously proposed (Schemes 5 and 6)[37,44,45] as primary reactions of **2** are thermodynamically less favorable.

Taking the solvation free energy into account does not change the picture significantly (Figure 6, red numbers). As mentioned above, **2** has been proposed to be the most important intermediate of the HNF decomposition in the melt.[37,44,45] However, our calculations demonstrate that **2** is thermodynamically very unfavorable in both the gas phase and melt. Apart from that, the decomposition of **2** through the elimination of NO_2 is a highly endothermic process. Even more favorable reactions of **2**, OH and NOOH elimination, have reaction enthalpies similar or higher than that of C−NO_2 bond cleavage of **1** (Figure 4). Therefore, our calculations do not support the assumption of Louwers et al.[37,45] (Scheme 6) as well as that of Sinditskii et al.[43,44] (Scheme 5). On the contrary, we can infer that the aci-form **2** does not play an important role in the thermolysis of HNF in both gas phase and melt.

Nitroform **1** was predicted to be a key intermediate of the HNF decomposition in the melt. The stepwise process starting from the decomposition of **H1** to **1** and **3** (Figure 3) and followed by NO_2 elimination from **1** (Figure 3) could be proposed. The enthalpy of this stepwise process in the melt was predicted to be 55.5 kcal/mol. Note that the effect of spin contamination is not significant in these calculations ($S^2 < 0.79$ for radical products).

We have also considered the reaction of NO_2 elimination from the salt **H1**. This reaction has been proposed to be the dominant primary reaction of HNF decomposition in the melt (Scheme 1, top).[24,25] The enthalpy of this reaction in the melt was calculated to be 63.7 kcal/mol. Therefore, calculations predict that this reaction is thermodynamically less favorable than the stepwise process. However, the wave function of the radical product of NO_2 elimination from **H1**, $(N_2H_5)^+(\cdot C(NO_2)_2)^-$, suffers from a significant degree of spin contamination ($S^2 \approx 0.95$ instead of 0.75). Therefore, it is clear that predicted value of the reaction enthalpy is overestimated. Therefore, the contribution of this channel to the HNF thermal decomposition could not be excluded.

On the basis of the results of our calculations, the following remarks on the mechanism of the HNF thermal decomposition can be made. First, although a shallow minimum corresponding to ionic salt exists on the PES of HNF, the activation barriers of its transformation are quite low. The salt is liable to the fast decomposition, preferably to nitroform **1** and hydrazine **3** in both gas phase and melt. The free energy of activation of this reaction is <10 kcal/mol. This fact agrees well with the absence of HNF among the gas-phase decomposition products.[30,31,44,45] The thermolysis of HNF in the gas phase and melt occurs mainly through the intermediacy of nitroform **1**; the computations do not support the suggestion[37,44,45] that the aci-nitroform **2** is an important intermediate of HNF decomposition. C−NO_2 bond cleavage was found to be the dominant reaction of the nitroform **1** decay.

Acknowledgment. Support of this work by the Siberian Supercomputer Center is gratefully acknowledged. V.G.K. appreciates the support of this work by the Russian Federal Agency of Education state contract (project NK-187P(1)) and by the INTAS (project YSF 06-1000014-6324). We are thankful to Prof. Valery Sinditskii for valuable discussions.

Supporting Information Available: Cartesian coordinates of all compounds under study. Stationary points on the PES for the primary stages of ANF thermal decomposition in the melt and gas phases. This material is available free of charge via the Internet at http://pubs.acs.org.

References and Notes

(1) Jacobs, P. W. M.; Whitehead, H. M. *Chem. Rev.* **1969**, *69*, 551.
(2) Brill, T. B.; Brush, P. J.; Patil, D. G. *Combust. Flame* **1993**, *94*, 70.
(3) Yuan, G.; Feng, R.; Gupta, Y. M.; Zimmerman, K. *J. Appl. Phys.* **2000**, *88*, 2371.
(4) Brill, T. B.; Brush, P. J.; Patil, D. J. *Combust. Flame* **1993**, *92*, 178.
(5) Korobeinichev, O. P.; Bolshova, T. A.; Paletsky, A. A. *Combust. Flame* **2001**, *126*, 1516.
(6) Mishra, I. B.; Russell, T. P. *Thermochim. Acta* **2002**, *384*, 47.
(7) Talawar, M. B.; Sivabalan, R.; Anniyappan, M.; Gore, G. M.; Asthana, S. N.; Gandhe, B. R. *Combust., Explos., Shock Waves* **2007**, *43*, 62.
(8) Oxley, J. C.; Smith, J. L.; Zheng, W.; Roger, E.; Coburn, M. D. *J. Phys. Chem. A* **1997**, *101*, 7217.
(9) Beckstead, M.; Puduppakkam, K.; Thakre, P.; Yang, V. *Prog. Energy Combust. Sci.* **2007**, *33*, 497.
(10) Santhosh, G.; Ghee, A. *J. Therm. Anal. Calorim.* **2008**, *94*, 263.
(11) Santhosh, G.; Ghee, A. *Thermochim. Acta* **2008**, *480*, 43.
(12) Fried, L.; Manaa, M.; Pagoria, P.; Simpson, R. *Annu. Rev. Mater. Res.* **2001**, *31*, 291.
(13) Pagoria, P.; Lee, G.; Mitchell, A.; Schmidt, R. *Thermochim. Acta* **2002**, *384*, 187.
(14) Göbel, M.; Klapötke, T. *Z. Anorg. Allg. Chem.* **2007**, *633*, 1006.
(15) Nguyen, M.-T.; Jamka, A. J.; Cazar, R. A.; Tao, F.-M. *J. Chem. Phys.* **1997**, *106*, 8710.
(16) Tao, F.-M. *J. Chem. Phys.* **1998**, *108*, 193.
(17) Snyder, J. A.; Cazar, R. A.; Jamka, A. J.; Tao, F.-M. *J. Phys. Chem. A* **1999**, *103*, 7719.
(18) Alkorta, I.; Rozas, I.; Yanez, O.; Elguero, J. *J. Phys. Chem. A* **2001**, *105*, 7481.
(19) Godfrey, J. N. U.S. Patent 3,196,059, July 20, 1965. CA 63:P8113g.
(20) Johnson, H.; Oja, P. D. U.S. Patent 3,213,609, Oct 26, 1965. CA 64:P3276d.
(21) Dickens, B. *Chem. Commun. (London)* **1967**, 246.
(22) Lovett, J. R. U.S. Patent 3,378,594, April 16, 1968. CA 68: P116121y.
(23) Dickens, B. *J. Res. Natl. Bur. Stands.* **1970**, *74A*, 309.
(24) McHale, E. T.; von Elbe, G. *Combust. Sci. Technol.* **1970**, *2*, 227.
(25) Von Elbe, G.; Levy, J.; Adams, S. Technical Report DA 36-034-AMC-0091R; Atlantic Research Corporation: Gainesville, VA, 1964.
(26) Koroban, V.; Smirnova, T. I.; Bashirova, T. N.; Svetlov, B. S. *Tr. Mosk. Khim.-Technol. Inst. im. D. I. Mendeleeva* **1979**, *104*, 38.
(27) Maslak, P.; Chapman, W. H., Jr. *J. Org. Chem.* **1990**, *55*, 6334.
(28) Zee, F. W.; Mul, J. M.; Hordijk, A. C. Technical Report C06B47/08, C01B21/16, International Patent, 1994.
(29) Schoyer, H. F.; Schnorhk, A. J.; Korting, P. A.; van Lit, P. J.; Mul, J. M.; Gadiot, G. M.; Meulenbrugge, J. J. *J. Propul. Power* **1995**, *11*, 856.
(30) Brill, T. B.; Arisava, H.; Brush, P. J.; Gongwer, P. E.; Williams, G. K. *J. Phys. Chem.* **1995**, *99*, 1384.
(31) Williams, G. K.; Brill, T. B. *Combust. Flame* **1995**, *102*, 418.
(32) Louwers, J.; van der Heijden, A. International Patent Application WO/99/59940, Nov 25, 1999.
(33) Louwers, J.; Gadiot, G. M.; Versluis, M.; Landman, A. J.; van der Meer T. H.; Roekarts, D. AIAA paper 98-3385. Proceedings of the 34th AIAA Joint Propulsion Conference and Exhibit, Cleveland, OH, July 13−15, 1998.

(34) de Klerk, W. P.; van der Heijden, A. E.; Veltmans, W. H. M. *J. Therm. Anal. Calorim.* **2001**, *64*, 973.
(35) Schoyer, H. F.; Welland-Veltmans, W. H.; Louwers, J.; Korting, P. A.; van der Heijden, A. E.; Keizers, H. L.; van den Berg, R. P. *J. Propul. Power* **2002**, *18*, 131.
(36) Scoyer, H. F.; Welland-Veltmans, W. H.; Louwers, J.; Korting, P. A.; van der Heijden, A. E.; Keizers, H. L.; van den Berg, R. P. *J. Propul. Power* **2002**, *18*, 138.
(37) Lowers, J. Combustion and Decomposition of Hydrazinium Nitroformate and HNF Propellants. Ph.D. Thesis, TU Delft: Delft, The Netherlands, 2000.
(38) Courtheoux, L.; Amariei, D.; Rossignol, S.; Kappenstein, C. *Appl. Catal., B* **2006**, *62*, 217.
(39) Frankel, M.; Gunderloy, F.; Woolery, D., II. U.S. Patent 4122124, Oct 24, 1978.
(40) Frankel, M.; Rainere, F.; Thompson, W.; Witucki, E.; Woolery, D., II. U.S. Patent 4147371, 1979.
(41) de Klerk, W. P.; Popescu, C.; Veltmans, W. H. M. *J. Therm. Anal. Calorim.* **2003**, *72*, 955.
(42) Ermolin, N. E. Z.; V, E.; Keizers, H. H. *Combust., Explos., Shock Waves* **2006**, *42*, 509.
(43) Sinditskii, V. P.; Egorshev V. Y.; Serushkin V. V.; Levchenkov, A. I. In *Proceedings of the 3rd International High Energy Materials Conference and Exhibit*, Thiruvananthapuram, India, 2000; p 489.
(44) Sinditskii, V. P.; Serushkin V. V.; Filatov, S. A.; Egorshev V. Y. In *Proceedings of the 5th International Symposium Special Topics in Chemical Propulsion*; Kuo, K. K., De Luca, L. T., Eds.; Stresa, Italy, 2000; p 576.
(45) Louwers, J.; Parr, T.; Hanson-Parr, D. AIAA paper 99-109137. AIAA Aerospace Sciences Meeting and Exhibit, Reno, NV, Jan 11−14, 1999.
(46) Nazin, G.; Manelis, G.; Dubovitskii, F. *Bull. Acad. Sci. USSR, Div. Chem. Sci.* **1969**, 945 (in orig. 1035).
(47) Mebel, A. M.; Lin, M. C.; Morokuma, K.; Melius, C. F. *J. Phys. Chem.* **1995**, *99*, 6842.
(48) Alavi, S.; Thompson, D. *J. Chem. Phys.* **2002**, *117*, 2599.
(49) Alavi, S.; Thompson, D. *J. Chem. Phys.* **2003**, *118*, 2599.
(50) Alavi, S.; Thompson, D. *J. Chem. Phys.* **2003**, *119*, 4274.
(51) Alavi, S.; Thompson, D. *J. Phys. Chem. A* **2004**, *108*, 8801.
(52) Gonzalez, C.; Schlegel, H. *J. Chem. Phys.* **1990**, *90*, 2154.
(53) Curtiss, L. A.; Raghavachari, K.; Redfern, P. C.; Rassolov, V.; Pople, J. A. *J. Chem. Phys.* **1998**, *109*, 7764.
(54) Kiselev, V. G.; Gritsan, N. P. *J. Phys. Chem. A* **2008**, *112*, 4458.
(55) Kiselev, V. G.; Gritsan, N. P. *J. Phys. Chem. A* **2009**, *113*, 3677.
(56) Cances, M. T.; Mennucci, B.; Tomasi, J. *J. Chem. Phys.* **1997**, *107*, 3032.
(57) Mennucci, B.; Tomasi, J. *J. Chem. Phys.* **1997**, *106*, 5151.
(58) Becke, A. D. *J. Chem. Phys.* **1993**, *98*, 5648.
(59) Lee, C.; Yang, W.; Parr, R. G. *Phys. Rev. B* **1988**, *37*, 785.
(60) Frisch, M. J. Trucks, G. W.; Schlegel, H. B.; Scuseria, G. E.; Robb, M. A.; Cheeseman, J. R.; Montgomery, J. A., Jr.; Vreven, T.; Kudin, K. N.; Burant, J. C.; Millam, J. M.; Iyengar, S. S.; Tomasi, J.; Barone, V.; Mennucci, B.; Cossi, M.; Scalmani, G.; Rega, N.; Petersson, G. A.; Nakatsuji, H.; Hada, M.; Ehara, M.; Toyota, K.; Fukuda, R.; Hasegawa, J.; Ishida, M.; Nakajima, T.; Honda, Y.; Kitao, O.; Nakai, H.; Klene, M.; Li, X.; Knox, J. E.; Hratchian, H. P.; Cross, J. B.; Bakken, V.; Adamo, C.; Jaramillo, J.; Gomperts, R.; Stratmann, R. E.; Yazyev, O.; Austin, A. J.; Cammi, R.; Pomelli, C.; Ochterski, J. W.; Ayala, P. Y.; Morokuma, K.; Voth, G. A.; Salvador, P.; Dannenberg, J. J.; Zakrzewski, V. G.; Dapprich, S.; Daniels, A. D.; Strain, M. C.; Farkas, O.; Malick, D. K.; Rabuck, A. D.; Raghavachari, K.; Foresman, J. B.; Ortiz, J. V.; Cui, Q.; Baboul, A. G.; Clifford, S.; Cioslowski, J.; Stefanov, B. B.; Liu, G.; Liashenko, A.; Piskorz, P.; Komaromi, I.; Martin, R. L.; Fox, D. J.; Keith, T.; Al-Laham, M. A.; Peng, C. Y.; Nanayakkara, A.; Challacombe, M.; Gill, P. M. W.; Johnson, B.; Chen, W.; Wong, M. W.; Gonzalez, C.; Pople, J. A. *Gaussian 03*, revision E.01; Gaussian, Inc.: Wallingford, CT, 2004.
(61) Curtiss, L. A.; Raghavachari, K.; Redfern, P. C. *J. Chem. Phys.* **1997**, *106*, 1063.
(62) Chase, M. W., Jr. *NIST-JANAF Themochemical Tables*, 4th ed.; Journal of Physical and Chemical Reference Data Monograph *9*; American Chemical Society: Washington, D.C., 1998.
(63) *NIST Chemistry WebBook*; Linstrom, P. J., Mallard, W. G., Eds.; NIST Standard Reference Database Number *69*; National Institute of Standards and Technology: Gaithersburg, MD, 2005. http://webbook.nist.gov/chemistry/.
(64) Miroshnichenko, E. A.; Lebedev, Y. A.; Shevelev, S. A.; Gulevskaya, V. I.; Fainzilberg, A. A.; Apin, A. Y. *Russ. J. Phys. Chem. (Transl. of Zh. Fiz. Khim.)* **1967**, *41*, 783. (1477 in original publication).
(65) McCullough, J. P.; Scott, D. W.; Pennington, R. E.; Hossenlopp, I. A.; Waddington, G. *J. Am. Chem. Soc.* **1954**, *76*, 4791.
(66) Lebedeva, N. D.; Ryadenko, V. L. *Russ. J. Phys. Chem. (Transl. of Zh. Fiz. Khim.)* **1973**, *47*, 1382. (2442 in original publication).
(67) Lebedev, V. M. E.; Matyushin, Y.; Larionov, V.; Romanov, V.; Bukolov, Y.; Denisov, G.; Balepin, A.; Lebedev, Y. *Russ. J. Phys. Chem. (Transl. of Zh. Fiz. Khim.)* **1975**, *49*, 1133. (1927 in original publication).
(68) Matus, M. H.; Arduengo, A. J.; Dixon, D. A. *J. Phys. Chem. A* **2006**, *110*, 10116.
(69) Konkova, T. S.; Matyushin, Y. N. *Russ. Chem. Bull.* **1998**, *47*, 2371.
(70) Gutowski, K. E.; Holbrey, J. D.; Rogers, R. D.; Dixon, D. A. *J. Phys. Chem. B* **2005**, *109*, 23196.
(71) Jenkins, H.; Roobottom, H.; Passmore, J.; Glasser, L. *Inorg. Chem.* **1999**, *38*, 3609.
(72) Jenkins, H.; Tudela, D.; Glasser, L. *Inorg. Chem.* **2002**, *41*, 2364.
(73) Gutowski, K.; Rogers, R.; Dixon, D. *J. Phys. Chem. B* **2007**, *111*, 4788.
(74) Miroshnichenko, E.; Lebedev, Y.; Apin, A. *Russ. J. Phys. Chem. (Transl. of Zh. Fiz. Khim.)* **1967**, *41*, 791. (1488 in original publication).
(75) Koppel, Il.; Burk, P.; Koppel, Iv.; Leito, I.; Sonoda, T.; Mishima, M. *J. Am. Chem. Soc.* **2000**, *122*, 5114.
(76) Pokon, E.; Liptak, M.; Feldgus, S.; Shields, G. *J. Phys. Chem. A* **2001**, *105*, 10483.
(77) Gutowski, K.; Dixon, D. *J. Phys. Chem. A* **2006**, *110*, 12044.

JP906853E